ARTICLES

A High-Resolution MAS NMR Study of the Structure of Fluorinated NiW/γ-Al_2O_3 Hydrotreating Catalysts

Weiping Zhang,† Mingyong Sun,‡ and Roel Prins*

Institute for Chemical and Bioengineering, Swiss Federal Institute of Technology (ETH), CH-8093, Zurich, Switzerland

Received: March 31, 2003; In Final Form: June 30, 2003

The structures of fluorinated oxidic and sulfided W/γ-Al_2O_3 and NiW/γ-Al_2O_3 catalysts were studied by means of multinuclear MAS NMR and BET measurements. The quantitative ^{1}H and ^{19}F MAS NMR results show that fluorination of γ-alumina favors the formation of polymeric tungstate in the catalysts and promotes the sulfidation of tungsten. Addition of tungsten to fluorinated γ-Al_2O_3 leads to the transformation of part of the type-S1 fluorine, bonded to one aluminum atom, to the type-S3 fluorine, bonded to three aluminum atoms. Sulfidation results in a reorganization of the hydroxyl groups on the surface of fluorinated alumina and in a partial hydrolysis of the alumina network because of the H_2O produced during sulfidation and the inductive effect of fluorine on the alumina lattice. Nickel reduces the NMR signal intensities in the oxidic samples because of its strong paramagnetic effect on the ^{1}H, ^{19}F, and ^{27}Al resonances. Sulfidation decreases the paramagnetic effect of nickel because of the combination of nickel with WS_2 into the Ni−W−S structure.

Introduction

Supported nickel (or cobalt) and molybdenum (or tungsten) are widely used as hydrotreating catalysts in oil refining. They are prepared in the oxidic form and then converted to the sulfidic form before application.[1,2] Alumina-supported nickel−tungsten (NiW) catalysts have a higher hydrogenation activity than molybdenum-based catalysts, but they are difficult to sulfide.[3,4] Considerable effort has been made to improve the performance of these catalysts, including the modification of the precursors with fluorine.[5−13] The effects of fluorine on alumina-supported hydrotreating catalysts have been ascribed to changes in the dispersion of the metal species in the catalyst precursor,[6] to an increase in the sulfidability of the metal oxide,[8] and to changes in the morphology of the metal sulfide on the alumina surface.[9] Our previous EXAFS, TPS, and XPS studies revealed that fluorination facilitates the sulfidation of tungsten,[11−13] while TEM revealed that it increased the proportion and stacking of WS_2 crystallites.[14]

The structure of the active species in sulfided catalysts determines their catalytic performance. However, few studies have concentrated on the structure of fluoride and how fluoride interacts with the support and active phase in hydrotreating catalysts. ^{19}F magic-angle spinning nuclear magnetic resonance (MAS NMR) distinguishes between different fluorine species in fluorinated amorphous alumina and aluminum oxophosphates when fast spinning rates are employed to average the large homo- and heteronuclei dipolar interactions in the solid samples.[15,16] High-resolution ^{1}H MAS NMR has been used extensively to investigate the hydroxyl groups in porous materials. In contrast to IR, NMR directly provides quantitative information about the changes in the number of hydroxyl groups in alumina, because it is unnecessary to determine extinction coefficients.[17,18] In this study, an ultrafast rate of sample spinning, up to 29.5 kHz, reduced most of the ^{19}F−^{19}F and ^{19}F−^{1}H dipolar interactions in the fluorinated γ-alumina support. The resulting high-resolution ^{19}F MAS NMR spectra were used to identify the distribution of fluorine species in NiW/γ-Al_2O_3F catalysts before and after sulfidation. Using this information and that obtained from ^{1}H MAS NMR, ^{27}Al MAS, and ^{1}H→^{27}Al cross-polarization MAS NMR, we studied the variations in the structures of NiW/γ-Al_2O_3F catalysts during preparation and sulfidation.

Experimental Section

Fluorinated alumina (Al_2O_3F) was prepared by impregnating γ-Al_2O_3 (Condea) with an aqueous solution of ammonium fluoride (Fluka) followed by drying at 393 K for 4 h and calcination at 773 K for 4 h in a stream of air at a heating rate of 2 K/min. The resulting fluoride content was 1.0 wt %, as measured by X-ray fluorescence spectroscopy. The alumina and fluorinated alumina were then loaded with W and NiW through the stepwise impregnation of ammonium metatungstate (Fluka) and nickel nitrate hexahydrate (Aldrich). The impregnated samples were dried and calcined after each impregnation, as described above for the preparation of fluorinated alumina. The resultant catalysts contained 5, 10, and 15 wt % of WO_3 and 1 wt % of NiO. All catalysts were sulfided in a quartz reactor in a mixture of 10 vol % H_2S/H_2. The gas flow was 150 mL/min;

* Corresponding author. Tel: 41-1-6325490; fax: 41-1-6321162; e-mail: prins@tech.chem.ethz.ch.

† Present address: Steacie Institute for Molecular Sciences, National Research Council of Canada, Ottawa, Ontario K1A 0R6, Canada.

‡ Present address: Department of Chemical and Materials Engineering, University of Alberta, Edmonton, Alberta T6G 2G6, Canada.

10.1021/jp030408t CCC: $25.00
Published on Web 09/12/2003

the catalysts were heated at a rate of 6 K/min to 673 K and were kept at this temperature for 4 h. After cooling to room temperature under flowing high-purity N_2, the samples were sealed in the reactor and transferred to a glovebox. They are referred to as *x*Ni *y*W/γ-Al_2O_3F−S, where *x* and *y* are the weight percentages of NiO and WO_3, respectively, and S stands for sulfidation. Prior to the $^1H\rightarrow^{27}Al$ cross-polarization magic-angle spinning (CP/MAS) NMR experiments, the samples were hydrated in a desiccator with a saturated NH_4NO_3 solution.[19] Before acquisition of the ^1H MAS NMR spectra, all the samples were degassed at 673 K and a pressure lower than 10^{-2} Pa for 10 h.

The surface areas and pore volumes of all the samples were measured at the temperature of liquid nitrogen (77 K) using a Micromeritics TriStar-3000 instrument. The samples were degassed at 673 K overnight before the measurements. The surface areas were calculated using the BET model, while the pore volumes were estimated from t-plot calculations.

All the NMR measurements were performed on a Bruker Avance-400 spectrometer at resonance frequencies of 376.5 MHz for ^{19}F, 400.2 MHz for ^1H, and 104.3 MHz for ^{27}Al. ^1H MAS NMR spectra were recorded using a single pulse ($\pi/4$, 2.2 μs) with a 4-s recycle delay and 400 scans. To obtain quantitative results, all the samples were weighed and the ^1H MAS NMR spectra calibrated by measuring a known amount of 1,1,1,3,3,3-hexafluoro-2-propanol (Fluka) under the same conditions.[18] ^{19}F MAS NMR experiments were carried out using 2.5-mm rotors at a spinning rate of 29.5 kHz, a recycle delay of 10 s, and 1600 scans. Spin−echo sequences ($\pi/2-\tau-\pi-\tau-$acquire) were applied to reduce the fluorine background that originated from the probe head. The excitation pulse length was 1.5 μs ($\pi/2$). By varying the τ value to acquire different spectra, it was found that when τ is 15 times the rotor period, that is, 508.47 μs, the strong fluorine signal from the probe head can be reduced strongly, and the line shape of the fluorine in the sample can be maintained as in the single-pulse sequence. ^{19}F chemical shifts were referenced to $CFCl_3$ at 0 ppm. For the quantitative determination of the fluorine species, all the samples were weighed and measured under the same conditions using the starting fluorinated alumina as the external standard. ^{27}Al MAS NMR spectra were collected under high-power proton decoupling using a 0.63 μs $\pi/12$ pulse with a 2-s recycle delay and 200 scans. To record $^1H\rightarrow^{27}Al$ CP/MAS spectra, an optimized contact time of 0.9 ms, a recycle delay of 2 s, and 10000−15000 scans were used. The Hartmann−Hahn condition was established as described in the literature.[19] Both the ^1H and ^{27}Al MAS NMR spectra were recorded using 4-mm ZrO_2 rotors and a spinning rate of 10 kHz; the chemical shifts were referenced to tetramethylsilane and to 1% aqueous $Al(H_2O)_6^{3+}$, respectively. The Dmfit98 program was employed for deconvolution and integration of the spectra using Gaussian−Lorentzian line shapes.[20] The fitting errors for our spectra were estimated to be about 5%.

Results

Surface Area and Pore Volume. Table 1 presents the BET surface areas and pore volumes of NiW/Al_2O_3F and NiW/Al_2O_3 catalysts, before and after sulfidation. Fluorination with 1.0-wt % fluoride hardly affected the surface area and pore volume of γ-Al_2O_3. Adding W and NiW to alumina and fluorinated alumina increased the surface area of the alumina support probably because of the extra surface area of WO_3. Meanwhile, the surface area increased more for the F-free than for the fluorinated alumina, but the pore volume decreased more for the fluorinated than for the F-free alumina. This indicates that fluoride induces the formation of polytungstates in the catalysts.[21] After sulfidation, the surface area and pore volume of the W and NiW catalysts hardly changed.

TABLE 1: Surface Areas and Pore Volumes of Supported NiW/Al_2O_3F, NiW/Al_2O_3 Catalysts before and after Sulfidation (per Gram of Al_2O_3)

sample	surface area (m^2/g)	pore volume (cm^3/g)
γ-Al_2O_3	216	0.41
1.0 F/Al_2O_3	215	0.41
5W/Al_2O_3F	218	0.41
10W/Al_2O_3F	217	0.36
10W/Al_2O_3	222	0.39
15W/Al_2O_3F	225	0.37
1Ni 10W/Al_2O_3F	219	0.39
1Ni 10W/Al_2O_3	220	0.37
10W/Al_2O_3F-S	217	0.38
10W/Al_2O_3-S	222	0.38
1Ni 10W/Al_2O_3F-S	217	0.41
1Ni 10W/Al_2O_3-S	219	0.37

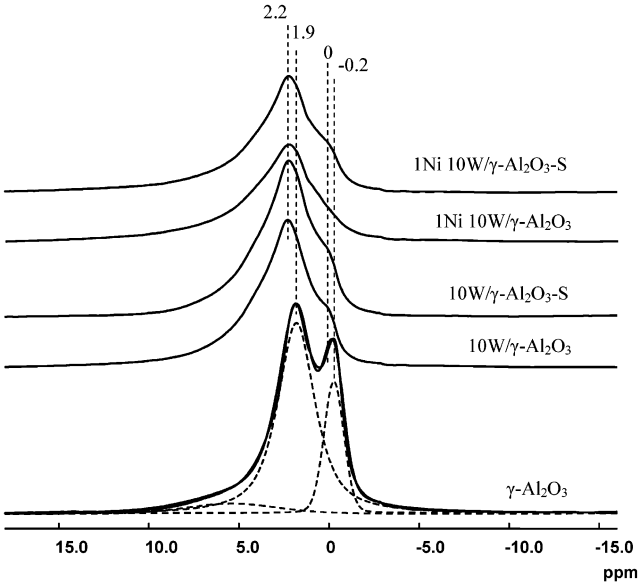

Figure 1. ^1H MAS NMR spectra of 10W/Al_2O_3 and 1Ni10W/Al_2O_3 before and after sulfidation, recorded with a sample spinning rate of 10 kHz and 400 scans.

^1H MAS NMR. Figure 1 shows the ^1H MAS NMR spectra of the W/γ-Al_2O_3 and NiW/γ-Al_2O_3 catalysts, before and after sulfidation. The spectrum of pure alumina shows two peaks at −0.2 and 1.9 ppm and a shoulder at around 5.2 ppm, which are attributed to basic hydroxyl groups, acidic hydroxyl groups, and residual water on the surface of alumina, respectively.[17,22,23] Quantitative analysis shows that there are far more acidic hydroxyls than basic hydroxyls (Table 2), indicating that the surface of alumina is more acidic than basic. The total amount of hydroxyls is 1.43 mmol/g on the F-free alumina. With a surface area of 216 m^2/g, this corresponds to 4 OH/nm^2, in agreement with the values (3−5 OH/nm^2) reported in the literature.[17,24,25] After impregnation of tungsten, the resonance positions of the basic and acidic hydroxyls shift slightly to low field. This suggests that the remaining surface hydroxyls are present in closed pores or as W−OH−Al bonds.[26] The total ^1H signal intensity decreases upon loading with W (Table 2), and the number of the basic hydroxyl groups decreases to a greater extent than that of the acidic hydroxyl groups. Subsequent impregnation with Ni does not affect the chemical shifts but causes a considerable decrease in the total signal intensity.

TABLE 2: Concentrations of Hydroxyls in Supported NiW/Al_2O_3, NiW/Al_2O_3F Catalysts before and after Sulfidation (mmol per Gram of Al_2O_3)

sample	amount of acidic hydroxyls	amount of basic hydroxyls	total amount of hydroxyls
γ-Al_2O_3	1.12	0.31	1.43
$10W/Al_2O_3$	0.43	0.06	0.49
$10W/Al_2O_3$-S	0.44	0.10	0.54
$1Ni\ 10W/Al_2O_3$	0.27	0.01	0.28
$1Ni\ 10W/Al_2O_3$-S	0.31	0.04	0.35
$1.0\ F/Al_2O_3$	0.90	0.03	0.93
$10W/Al_2O_3F$	0.29	0.02	0.31
$10W/Al_2O_3F$-S	0.41	0.04	0.45
$1Ni\ 10W/Al_2O_3F$	0.16	0.01	0.17
$1Ni\ 10W/Al_2O_3F$-S	0.25	0.02	0.27

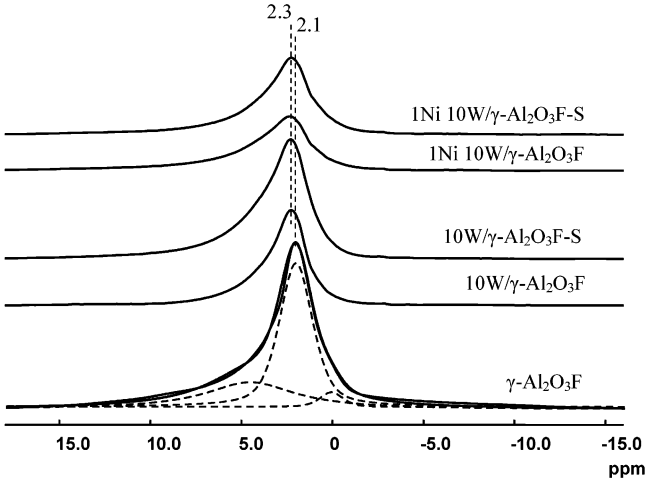

Figure 2. ^1H MAS NMR spectra of $10W/Al_2O_3F$ and $1Ni10W/Al_2O_3F$ before and after sulfidation, recorded with a sample spinning rate of 10 kHz and 400 scans.

Sulfidation of W/Al_2O_3 and NiW/Al_2O_3 catalysts increases the number of both the acidic and basic hydroxyls.

Upon fluorination of the alumina, the signal of the basic hydroxyls is reduced more readily than that of the acidic hydroxyls (Figure 2). This suggests that fluoride replaces the acidic and basic alumina hydroxyl groups at the same time but that the basic hydroxyl groups are substituted preferentially. Quantitative results show that the amount of surface hydroxyl groups decreases to 0.93 mmol/g at fluoride loading of 1.0 wt % (Table 2). The number of lost hydroxyl groups matches the number of adsorbed fluoride ions. This indicates that one fluoride substitutes one hydroxyl group without breaking the bridging Al−O−Al bonds when the fluoride content is as low as 1.0 wt %.[27] Furthermore, the residual acidic and basic hydroxyls shift to lower field, to 2.1 and 0.1 ppm, respectively (Figure 2), because of the inductive through-lattice effect of the electronegative fluoride.[22] After impregnating the fluorinated alumina with W or NiW, the positions of the acidic and basic hydroxyls shift even further, and their numbers decrease. Subsequent sulfidation increases the number of the acidic and basic hydroxyl groups, however. The total number of hydroxyls increases to a greater extent on the fluorinated alumina than on the F-free alumina.

^{19}F MAS NMR. Figure 3 shows the ^{19}F MAS NMR spectra of fluorinated Al_2O_3 with different tungsten loadings. Three bands can be distinguished at about −161 ppm (S1), −145 ppm (S2), and −132 ppm (S3), which are assigned to fluorine species bound to one, two, and three octahedral aluminum atoms, respectively.[27] At our loading of 1.0 wt % fluorine, aluminum

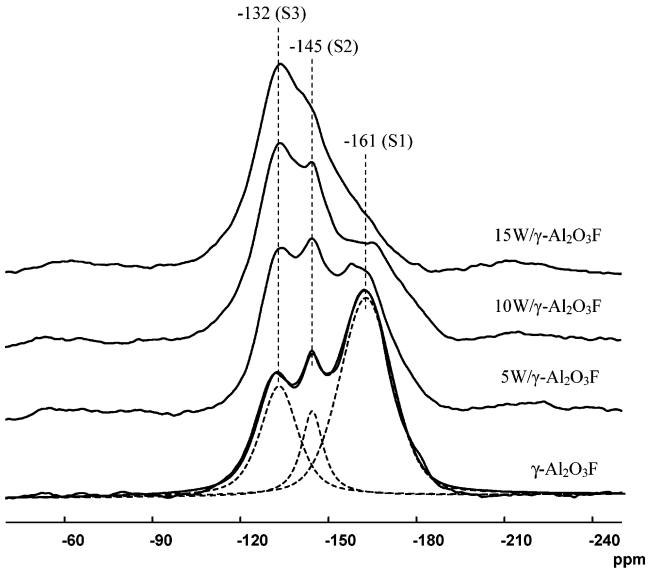

Figure 3. ^{19}F MAS NMR spectra of γ-Al_2O_3F supported with different W loadings, recorded with ultrafast spinning rate of 29.5 kHz and 1600 scans. The ^{19}F MAS NMR spectrum of γ-Al_2O_3F can be decomposed into three Gaussian−Lorentzian lines.

TABLE 3: Concentrations of Different Fluorine Species in Supported NiW/Al_2O_3F Catalysts before and after Sulfidation (mmol per Gram of Al_2O_3)

sample	*S*1	*S*2	*S*3	partially hydrolyzed fluorine species	total
Al_2O_3F	0.31	0.08	0.14	0	0.53
$5W/Al_2O_3F$	0.24	0.12	0.17	0	0.53
$10W/Al_2O_3F$	0.15	0.13	0.24	0	0.52
$15W/Al_2O_3F$	0.06	0.13	0.31	0	0.50
$10W/Al_2O_3F$-S	0.09	0.10	0.19	0.12	0.50
$15W/Al_2O_3F$-S	0.05	0.12	0.23	0.11	0.51
$1Ni\ 10W/Al_2O_3F$	0.10	0.09	0.12	0	0.31
$1Ni\ 15W/Al_2O_3F$	0.05	0.04	0.13	0	0.22
$1Ni\ 10W/Al_2O_3F$-S	0.08	0.10	0.14	0.09	0.41
$1Ni\ 15W/Al_2O_3F$-S	0.04	0.03	0.18	0.06	0.31

trifluoride was not observed. After impregnation of tungsten, the ^{19}F MAS NMR does not indicate the presence of W−F bonds. Such bonds should give signals 310 ppm downfield of Al−F species, since WF_6 is characterized by a resonance at 166 ppm lower field than CCl_3F.[28] It seems that fluorine interacts preferentially and strongly with the alumina surface. Quantitative decomposition and integration of the spectra led to the concentrations of the S1, S2, and S3 fluorine species listed in Table 3. The S1 species are predominant in the fluorinated alumina. With increasing tungsten loading, the amount of type S1 fluorine decreases considerably, while the amount of type S3 increases and that of type S2 is more or less constant. The total amount of fluorine hardly changes when the tungsten loading increases from 0 to 15 wt %. After adding the Ni promoter and sulfidation,^{19}F MAS NMR spectra were obtained as shown in Figures 4 and 5. As well as the three signals of the S1, S2, and S3 fluorine species, a new signal appeared at about −175 ppm for the sulfided catalysts, which may be due to hydrolyzed aluminum fluoride, for example, $Al(OH)_{3-x}F_x \cdot nH_2O$.[27,29]

Table 3 presents the results of the quantitative analysis of the fluorine species in the W/Al_2O_3F and NiW/Al_2O_3F samples. After sulfidation of the W/Al_2O_3F catalysts, the numbers of the S1, S2, and S3 fluorine species decrease, but the total number of fluorine species hardly changes because of the formation of the hydrolyzed aluminum fluoride. After adding Ni to W/Al_2O_3F, the numbers of the S1, S2, and in particular S3 fluorine species

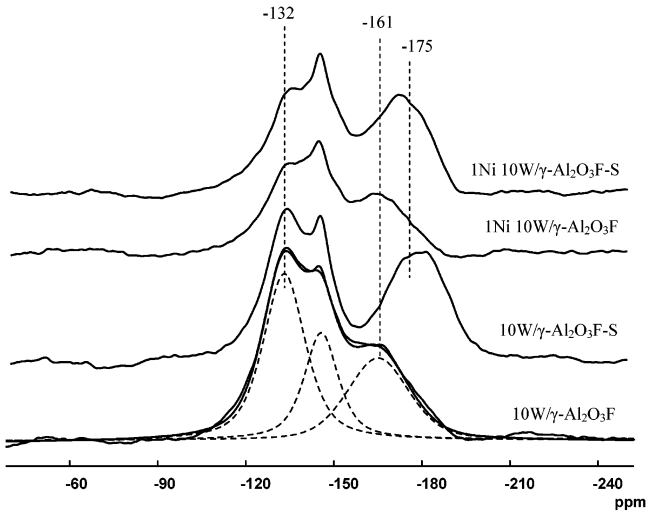

Figure 4. ^{19}F MAS NMR spectra of 10W/Al_2O_3F and 1Ni10W/Al_2O_3F before and after sulfidation, recorded with ultrafast spinning rate of 29.5 kHz and 1600 scans.

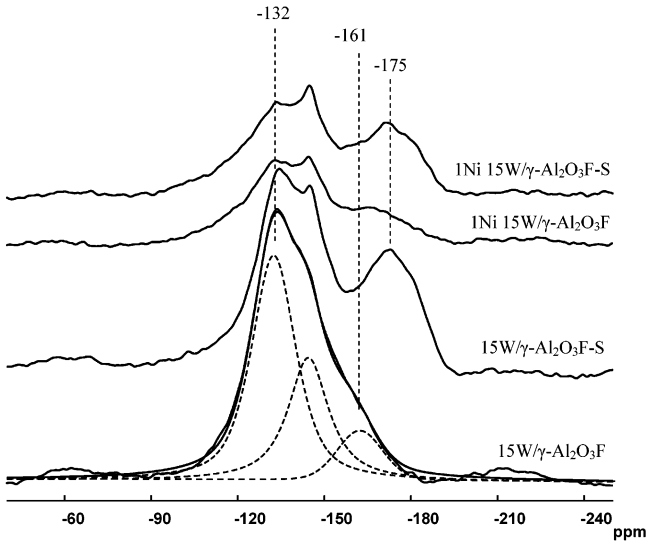

Figure 5. ^{19}F MAS NMR spectra of 15W/Al_2O_3F and 1Ni15W/Al_2O_3F before and after sulfidation, recorded with ultrafast spinning rate of 29.5 kHz and 1600 scans.

decrease substantially, and the total number of fluorine species decreases accordingly. After sulfidation of the NiW/Al_2O_3F catalysts, the total number of fluorine species increases again, mainly because of the formation of hydrolyzed aluminum fluoride and a slight increase in the number of the S3 species. Nevertheless, the total number of fluorine species in sulfided NiW/Al_2O_3F catalysts does not reach the level of the Ni-free catalysts. The concentration of hydrolyzed aluminum fluoride in the sulfided W/Al_2O_3F and NiW/Al_2O_3F catalysts is about 20%. Thus, aluminum fluoride species on the surface of alumina are partially hydrolyzed during sulfidation.

^{27}Al MAS and ^{1}H→^{27}Al CP/MAS NMR. ^{27}Al MAS NMR can yield information about the coordination of the aluminum atoms in γ-alumina. The ^{1}H→^{27}Al cross-polarization technique can selectively enhance the Al signals of aluminum atoms which are coupled with protons of neighboring hydroxyls.[30] Figure 6 shows the ^{27}Al MAS NMR spectra of W/Al_2O_3F and NiW/Al_2O_3F before and after sulfidation. As expected, there are two main signals, that at 65 ppm is due to four-coordinated aluminum and the other at 6 ppm is due to six-coordinated aluminum. All spectra are similar and correspond to that of the

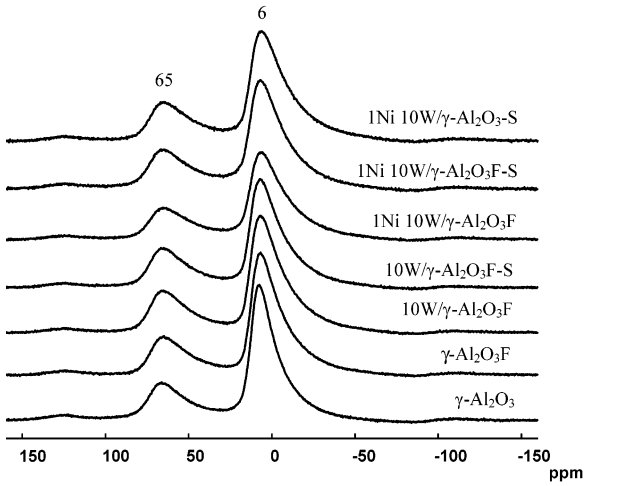

Figure 6. ^{27}Al MAS NMR spectra of 10W/Al_2O_3F and 1Ni10W/Al_2O_3F before and after sulfidation.

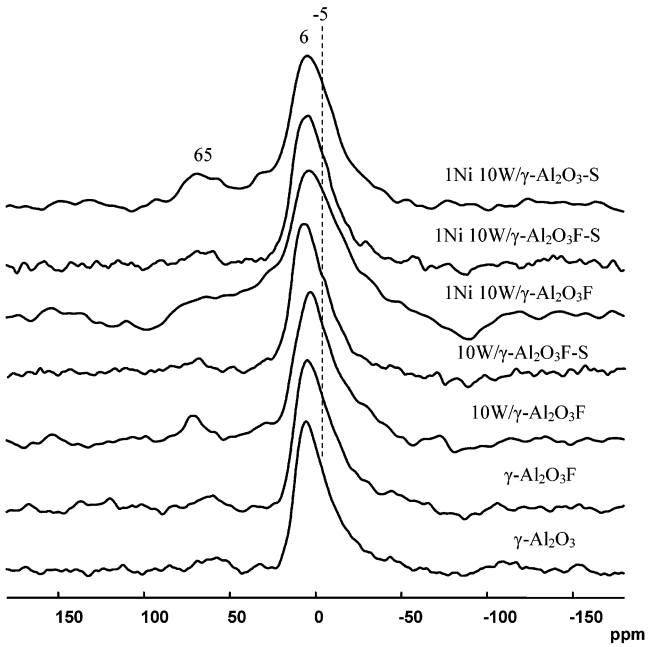

Figure 7. ^{1}H→^{27}Al MAS NMR spectra of 10W/Al_2O_3F and 1Ni10W/Al_2O_3F before and after sulfidation. The number of scans for 1Ni10W/Al_2O_3F is 39 k, others are 10−15 k.

original alumina; after introducing Ni, however, the ^{27}Al signal intensity decreases substantially, as observed in the ^{19}F and ^{1}H MAS NMR spectra. In the corresponding ^{1}H→^{27}Al cross-polarization MAS NMR spectra (Figure 7), the signal at 6 ppm is increased considerably compared to that at 65 ppm. This shows that the hydroxyl groups in the alumina are mainly connected to six-coordinated aluminum. Moreover, after ^{1}H→^{27}Al cross-polarization, a shoulder at about −5 ppm is enhanced in the sulfided samples. This may be due to the appearance of partially hydrolyzed aluminum fluoride after sulfidation.

Discussion

The quantitative analysis of the ^{1}H MAS NMR spectra showed that the number of surface hydroxyls decreased upon fluorination of alumina and that the decrease corresponds to the number of added fluoride ions. This indicates that one hydroxyl is displaced by one fluoride. Meanwhile, three signals were observed in the ^{19}F MAS NMR spectrum of fluorinated alumina. In our preceding study,[27] we ascribed these three

SCHEME 1: Three Types of Fluorine Species on the Surface of Fluorinated γ-Alumina

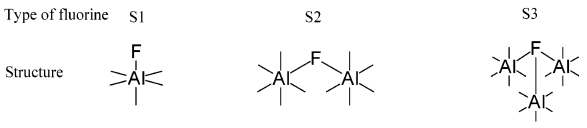

signals to the structures indicated in Scheme 1, analogous to the model of Knözinger and Ratnasamy for surface OH groups.[24] After the addition of 5 wt % WO_3, the intensity of the S1 signal decreased and that of the S2 and S3 signals increased. Further addition of tungsten decreased the intensity of the S1 signal and increased that of the S3 signal considerably, while the intensity of the S2 signal remained about constant and the total fluorine intensity did not change. This suggests that some of the type-S1 fluorine was transformed to type-S2 fluorine during catalyst preparation in aqueous solution and some of the type-S2 to type-S3 fluorine, while the total number of fluoride ions remained constant. In a solution of ammonium metatungstate, tungsten is present as tetrahedral WO_4^{2-} at high pH and as octahedral polytungstate at low pH. However, the surface tungsten species in a WO_3/Al_2O_3 catalyst consists solely of tetrahedral WO_4^{2-} complex anions at a low loading of WO_3 ($<15\%$).[31] Increasing the WO_3 loading will lead to the formation of polytungstate species. Since the tungsten loadings in our samples are smaller than 15 wt % WO_3, we do not expect polytungstate to be present in the nonfluorinated samples. The fluorination of the alumina support leads to the formation of polytungstate at lower tungsten loadings because of the loss of surface OH groups, but the major part of tungsten on the catalyst surface is still present as WO_4^{2-} species.[21] Therefore, we assume that following impregnation and calcination at 773 K the tungsten is present mainly as WO_4^{2-} on the alumina surface. Impregnation of F-free alumina with 10 wt % WO_3 resulted in a reduction of 0.94 mmol/g in the total number of hydroxyls, which is equal to twice the number of the added tungsten species (Table 2). This demonstrates that one WO_4^{2-} anion binds to two hydroxyls on the surface of alumina during the preparation of the catalysts. Concurrent with the consumption of hydroxyl groups, a rearrangement of the fluoride ions from type I to type III takes place.

Scheme 2 suggests how a WO_4^{2-} anion may become attached to the fluorinated alumina surface. According to Nortier et al.,[33,34] the most abundant face on the surface of γ-alumina is the (110) face. At low fluoride loading, the initial structure in Scheme 2 may be presented on the spinel lattice parallel to the (110) plane. When tungsten is impregnated on the fluorinated alumina, WO_4^{2-} anions may react with the sites adjacent to the Al−F species; double binding of the tungsten to the surface favors a change in the fluorine from type S1 to S3 (from structure 2 to 3 in Scheme 2). After sulfidation, the total amount of hydroxyls increased and the amount of acidic hydroxyls increased to a greater extent than that of the basic hydroxyls on the fluorinated alumina (Table 2). This implies that, during sulfidation of a fluorine-containing catalyst, the W−O−Al linkages break to give W−S instead of W−O bonds, since the Al−S bond is weak. As a result, type I sites become free again. At the same time, a reorganization of the hydroxyls from basic type I to acidic type III may occur (from structure 4 to 5 in Scheme 2). Sulfidation at 673 K of calcined alumina-supported tungsten catalysts can only convert about 50% tungsten to WS_2, and oxysulfides are formed before the formation of WS_2 at medium temperature (between 400 and 600 K). Structure 5 represents the oxysulfide intermediate of sulfidation, as identified by EXAFS.[11] However, in the presence of steam in the product

SCHEME 2: Proposed Mechanism for the Variations of the Structures on the Fluorinated γ-Alumina Surface upon Tungsten Incorporation and Sulfidation

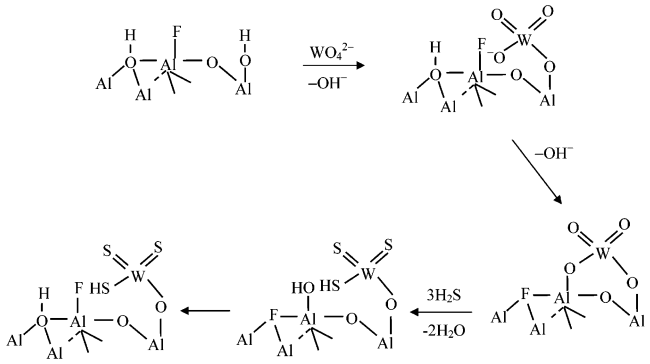

and fluoride on the alumina surface, reorganization of the hydroxyls at elevated temperature (673 K) may lead to the partial hydrolysis of the alumina network, as proven by the ^{19}F MAS NMR spectra of the sulfided samples.

Impregnation of the fluorinated alumina with 10 wt % WO_3 led to a reduction of 0.62 mmol/g in the total number of hydroxyls, which is less than twice the number of added tungsten species. The ^{19}F MAS NMR results show that there is no obvious loss of fluorine during impregnation of the fluorinated alumina (Table 3). Thus, fluorination of alumina leads to the formation of polymeric tungstate in the catalysts. This is consistent with the results of the BET measurements. After sulfidation, the increase in the total amount of hydroxyls on the $10W/Al_2O_3F$ catalyst is 0.14 mmol/g, which is larger than that on the $10W/Al_2O_3$ catalyst (0.05 mmol/g, cf. Table 2). This demonstrates that the addition of fluoride facilitates the sulfidation of tungsten, which is in agreement with our EXAFS results.[13]

The intensities of the ^1H NMR, ^{19}F NMR, and ^{27}Al NMR signals of the oxidic $NiW/Al_2O_3(F)$ sample were very low compared with those of the oxidic $W/Al_2O_3(F)$ sample. A reduction in signal intensity due to the presence of nickel was also observed in ^{31}P NMR investigations of phosphate-containing NiP/Al_2O_3[33,34] and $NiMoP/Al_2O_3$[35] samples. Nickel ions are paramagnetic; when a paramagnetic ion is near the NMR nucleus, a loss of signal may occur.[36] A reduction in the signal intensity, induced by paramagnetic interactions, has been used to estimate the proximity of the various compounds to Co or Ni and, thus, to obtain information about the distribution of these compounds.[35] In our case, the strong reduction in the ^1H NMR and ^{19}F NMR signals implies that the nickel cations are well dispersed and in the vicinity of fluoride ions and hydroxyl groups in the oxidic state. After sulfidation, the ^1H, ^{19}F, and ^{27}Al signal intensities increased considerably. This means that sulfidation reduces the paramagnetic effect of nickel. Thus, nickel is no longer well dispersed but is present in a segregated sulfidic state, which may be the Ni−W−S state, analogous to the Co−Mo−S and Ni−Mo−S phases.[37,38] The formation of a Ni−W−S phase, after decorating the edges of stacked WS_2 slabs with Ni atoms, may keep nickel away from the surface of the alumina support, thus reducing the paramagnetic effect of nickel.

Conclusions

Fluorination of γ-alumina promotes the formation of polymeric tungstates in the catalysts and also facilitates the sulfidation of tungsten. Impregnation of tungsten in the fluorinated alumina support leads to the transformation of type-S1 to type-S3 fluorine. Tungsten in the WO_3/Al_2O_3F catalyst may prefer-

entially react with hydroxyl groups on the alumina support, which are adjacent to type-S1 fluorine. Sulfidation results in a reorganization of the surface hydroxyls and a partial hydrolysis of the alumina network because of the formation of H_2O during sulfidation and the inductive effect of fluorine on the alumina lattice. In oxidic nickel-containing catalysts, the ^{1}H, ^{19}F, and ^{27}Al NMR signals decreased because of the proximity of paramagnetic nickel cations. Sulfidation eliminates the shielding effect of nickel on fluorine by separating nickel from fluorine to form the Ni−W−S phase.

References and Notes

(1) Topsøe, H.; Clausen, B. S.; Massoth, F. E. *Hydrotreating Catalysis*; Springer-Verlag: Berlin, 1996.
(2) Prins, R. *Adv. Catal.* **2001**, *46*, 399.
(3) Furimsky, E. *Catal. Rev.—Sci. Eng.* **1980**, *22*, 371.
(4) Scheffer, B.; Mangnus, P. J.; Moulijn, J. A. *J. Catal.* **1990**, *121*, 18.
(5) Boorman, P. M.; Kydd, R. A.; Sarbak, Z.; Somogyvari, A. *J. Catal.* **1987**, *106*, 544.
(6) Papadopoulou, Ch.; Lycourghiotis, A.; Grange, P.; Delmon, B. *Appl. Catal.* **1988**, *38*, 255.
(7) Matralis, H. K.; Lycourghiotis, A.; Grange, P.; Delmon, B. *Appl. Catal.* **1988**, *38*, 273.
(8) Benitez, A.; Ramirez, J.; Fierro, J. L. G.; Lopez Agudo, A. *Appl. Catal. A* **1996**, *144*, 343.
(9) Benitez, A.; Ramirez, J.; Vazquez, A.; Acosta, D.; Lopez Agudo, A. *Appl. Catal.* **1995**, *133*, 103.
(10) Kwak, C.; Lee, J. J.; Bae, J. S.; Choi, K.; Moon, S. H. *Appl. Catal. A* **2000**, *200*, 233.
(11) Sun, M.; Burgi, Th.; Cattaneo, R.; Prins, R. *J. Catal.* **2001**, *197*, 172.
(12) Sun, M.; Burgi, Th.; Cattaneo, R.; van Langeveld, A. D.; Prins, R. *J. Catal.* **2001**, *201*, 258.
(13) Schwartz, V.; Sun, M.; Prins, R. *J. Phys. Chem. B* **2002**, *106*, 2597.
(14) Sun, M.; Kooyman, P. J.; Prins, R. *J. Catal.* **2002**, *206*, 368.
(15) Harris, R. K.; Jackson, P. *Chem. Rev.* **1991**, *91*, 1427.
(16) Miller, J. M. *Prog. Magn. Reson. Spectrosc.* **1996**, *28*, 255.
(17) Jacobsen, C. J. H.; Topsøe, N. Y.; Topsøe, H.; Kellberg, L.; Jakobsen, H. J. *J. Catal.* **1995**, *154*, 65.
(18) Kraus, H.; Prins, R. *J. Catal.* **1996**, *164*, 260.
(19) Zhang, W.; Ma, D.; Han, X.; Liu, X.; Bao, X.; Guo, X.; Wang, X. *J. Catal.* **1999**, *188*, 393.
(20) Massiot, D.; Fayon, F.; Capron, M.; King, I.; Alonso, S. B.; Durand, J.-O.; Bujoli, B.; Gan, Z.; Hoatson, G. *Magn. Reson. Chem.* **2002**, *40*, 70.
(21) Cordero, R. L.; Solis, J. R.; Ramos, J. V. G.; Patricio, A. B.; Agudo, A. L. *Stud. Surf. Sci. Catal.* **1993**, *75*, 1928.
(22) DeCanio, E. C.; Edwards, J. C.; Bruno, J. W. *J. Catal.* **1994**, *148*, 76.
(23) Hunger, M.; Freude, D.; Pfeifer, H. *J. Chem. Soc., Faraday Trans.* **1991**, *87*, 657.
(24) Knözinger, H.; Ratnasamy, P. *Catal. Rev.—Sci. Eng.* **1978**, *17*, 31.
(25) Miciukiewicz, J.; Quader, Q.; Massoth, F. E. *Appl. Catal.* **1989**, *49*, 247.
(26) Mastikhin, V. M.; Nosov, A. V.; Terskikh, V. V.; Zamaraev, K. I.; Wachs, I. E. *J. Phys. Chem.* **1994**, *98*, 13621.
(27) Zhang, W.; Sun, M.; Prins, R. *J. Phys. Chem. B* **2002**, *106*, 11805.
(28) Arnaudet, L.; Bougon, R.; Buu, B.; Lance, M.; Nierlich, M.; Thuery, P.; Vigner, J. *J. Fluorine Chem.* **1995**, *71*, 123.
(29) Fischer, L.; Harlé, V.; Kasztelan, S.; d'Espinose de la Caillerie, J. B. *Solid State Nucl. Magn. Reson.* **2000**, *16*, 85.
(30) Morris, H. D.; Ellis, P. D. *J. Am. Chem. Soc.* **1989**, *111*, 6045.
(31) Salvati, L., Jr.; Makovsky, L. E.; Stencel, J. M.; Brown, F. R.; Hercules, D. M. *J. Phys. Chem.* **1981**, *85*, 3700.
(32) Nortier, P.; Fourre, P.; Mohammed Saad, A. B.; Saur, O.; Lavalley, J. C. *Appl. Catal.* **1990**, *61*, 141.
(33) Mohammed Saad, A. B.; Ivanov, V. A.; Lavalley, J. C.; Nortier, P.; Luck, F. *Appl. Catal.* **1993**, *94*, 71.
(34) DeCanio, E. C.; Edwards, J. C.; Scalzo, T. R.; Storm, D. A.; Bruno, J. W. *J. Catal.* **1991**, *132*, 498.
(35) Kraus, H.; Prins, R. *J. Catal.* **1997**, *170*, 20.
(36) La Mar, G. N.; Horrocks, W. D., Jr.; Holm, R. H. *NMR of Paramagnetic Molecules*; Academic Press: New York, 1973, Chapter 1.
(37) Wivel, C.; Candia, R.; Clausen, B. S.; Mørup, S.; Topsøe, H. *J. Catal.* **1981**, *68*, 453.
(38) Topsøe, H.; Clausen, B. S. *Appl. Catal.* **1986**, *25*, 273.